CRYSTAL GROWTH & DESIGN
2007
VOL. 7, NO. 3
521−525

Polymorphism in $Li_2Mo_4O_{13}$ Revisited

Jared P. Smit, Peter C. Stair, and Kenneth R. Poeppelmeier*

Department of Chemistry, Northwestern University, 2145 Sheridan Road, Evanston, Illinois 60208

Received August 29, 2006; Revised Manuscript Received September 30, 2006

ABSTRACT: The structure of *M*-$Li_2Mo_4O_{13}$ has been determined. *M*-$Li_2Mo_4O_{13}$ crystallizes in the monoclinic and noncentrosymmetric space group $P2_1$ (No. 4) with cell parameters $a = 8.2178(5)$ Å, $b = 21.2814(13)$ Å, $c = 8.5950(5)$ Å, $\beta = 96.0880(10)°$, $Z = 2$, and final residuals of R1 = 0.0225 and wR2 = 0.0536. *M*-$Li_2Mo_4O_{13}$ is one of three polymorphs and all three phases are Li−Mo cosubstituted V_6O_{13} homeotypes built on an identical oxygen-deficient cubic close-packed oxygen framework.

1. Introduction

An extensive study of the Li_2MoO_4−MoO_3 system reported both a high (*H*) and low (*L*) temperature phase of $Li_2Mo_4O_{13}$.[1] The *H* and *L* structural variations, which are closely related,[2,3] belong to the triclinic space group $P\bar{1}$ (No. 2). The cell parameters for *H*-$Li_2Mo_4O_{13}$ are $a = 8.612$ Å, $b = 11.562$ Å, $c = 8.213$ Å, $\alpha = 94.45°$, $\beta = 96.38°$, $\gamma = 111.24°$, and $Z = 3$, while the cell parameters for *L*-$Li_2Mo_4O_{13}$ are $a = 8.578$ Å, $b = 11.450$ Å, $c = 8.225$ Å, $\alpha = 109.24°$, $\beta = 96.04°$, $\gamma = 95.95°$, and $Z = 3$. The two compounds are homeotypes of the vanadium oxide V_6O_{13},[4] and the structural relationship and transformation of *L*-$Li_2Mo_4O_{13}$ into *H*-$Li_2Mo_4O_{13}$ has been described.[2,3]

During the preparation of *L*-$Li_2Mo_4O_{13}$, the authors noted the presence of two unusual crystals that were different from both the *H* and *L* phases.[3] Referred to as *M*-$Li_2Mo_4O_{13}$, the cell parameters were obtained; however, the crystals transformed to the more stable *H*-$Li_2Mo_4O_{13}$ before they could be further investigated, and its structure has not been determined. In this work, a high yield synthesis and complete crystal structure of *M*-$Li_2Mo_4O_{13}$ are reported, and the structural relationships are discussed. The three $Li_2Mo_4O_{13}$ polymorphs are cosubstituted homeotypes of V_6O_{13}, each reflecting a unique distribution of the lithium and the molybdenum cations.

While V_6O_{13} is often viewed as a shear structure derived from V_2O_5 in the $M_{3n}O_{8n-3}$ ($n = 2$) homologous series of phases, the crystallographic shear plane is part of a cubic close-packed oxygen lattice with regular oxygen vacancies. V_6O_{13} and the three $Li_2Mo_4O_{13}$ polymorphs are all built up from an oxygen-deficient close-packed array, and the latter are differentiated by three distinct occupation patterns of the octahedral sites.

2. Experimental Section

2.1. Materials and Synthesis. All starting materials were purchased from commercial suppliers and used without further purification. A mixture of 0.54 g of Li_2CO_3 (99+%, Sigma-Aldrich), 0.59 g of TiO_2 (anatase, 99.9+%, Sigma-Aldrich), and 3.19 g of MoO_3 (99.95%, Alfa Aesar), corresponding to a nominal stoichiometry of "$Li_2TiMo_3O_{12}$", was ground in an agate mortar, packed into a platinum crucible, and heated at a rate of 10 °C·min^{-1} to 635 °C. It was held at 635 °C for 1 h and then cooled slowly at a rate of 0.1 °C·min^{-1} to 525 °C, at which point the furnace was turned off. Colorless crystals were formed in good yield on top of the melt. ICP elemental analysis was performed with a VISTA-MPX Spectrometer. Although Ti^{4+} ions were present in the melted liquid composition, ICP elemental analysis showed no titanium in the resultant crystals. In contrast, a nominal melt stoichiometry of "$Li_2HfMo_3O_{12}$" resulted in crystals of $Li_{2.82}Hf_{0.795}(MoO_4)_3$ that adopt the lyonsite structure type,[5] perhaps reflecting the difference between the acid−base character of TiO_2 and HfO_2.

Table 1. Crystallographic Information for *M*-$Li_2Mo_4O_{13}$[a]

chemical formula	$Li_6Mo_{12}O_{39}$
formula weight	1816.92
crystal system	monoclinic
space group	$P2_1$
a	8.2178(5) Å
b	21.2814(13) Å
c	8.5950(5) Å
β	96.0880(10)°
V	1494.67(16) Å^3
Z	2
D_{calc}	4.037 Mg·m^{-3}
μ (Mo Kα)	4.989 mm^{-1}
Flack parameter	0.00(5)
R1 [$I > 2\sigma(I)$], R1 [all data]	0.0225, 0.0250
wR2 [$I > 2\sigma(I)$], wR2 [all data]	0.0536, 0.0547

[a] $R1 = \sum|F_o| - |F_c|/\sum|F_o|$. $wR2 = [\sum w(F_o^2 - F_c^2)^2/\sum w(F_o^2)^2]^{1/2}$.

2.2. Crystallography. A colorless crystal was mounted on a glass fiber for study by single-crystal X-ray diffraction. Measurements were made on a Bruker Smart 1000 equipped with CCD detector and graphite monochromated Mo Kα radiation and integrated with the SAINT-Plus program.[6] Details of the structure determination are listed in Table 1, and the atomic positions and displacement parameters for *M*-$Li_2Mo_4O_{13}$ are listed in Table S1 of the Supporting Information. A face-indexed absorption correction was applied using XPREP, followed by the SADABS program.[7] Systematic absences determined unambiguously the space group to be $P2_1$, and a check for missing symmetry was performed using PLATON.[8] The Flack parameter indicates the correct noncentrosymmetric absolute configuration. The structure was solved by direct methods and refined by full-matrix least-squares against F^2 using SHELXTL software.[9] Refinement of the molybdenum and oxygen atomic positions and anisotropic displacement parameters, and lithium atomic positions and isotropic displacement parameters, led to the final residuals. Further details of the crystal structure investigation can be obtained from the CIF in the Supporting Information or from the Fachinformationszentrum Karlsruhe, 76344 Eggenstein-Leopoldshafen, Germany (fax, (+49)7247-808-666; e-mail, crysdata@fiz-karlsruhe.de) on quoting the depository number CSD-416695.

3. Results and Discussion

3.1. Description of the Structure of M-$Li_2Mo_4O_{13}$. The structure of *M*-$Li_2Mo_4O_{13}$ is depicted in Figure 1. The asymmetric unit consists of 6 unique lithium positions, 12 unique molybdenum positions, and 39 unique oxygen positions. *M*-$Li_2Mo_4O_{13}$ is a layered structure with alternating single and double sheets of edge-sharing LiO_6 and MoO_6 octahedra. The single sheet is shown in Figure 2 and is built up from ordered rows of edge-sharing lithium- and molybdenum-centered octahedra, where every third octahedral position is empty. A row of two-

* To whom correspondence should be addressed. E-mail: krp@northwestern.edu. Tel.: 847-491-3505.

10.1021/cg060576l CCC: $37.00
Published on Web 02/01/2007

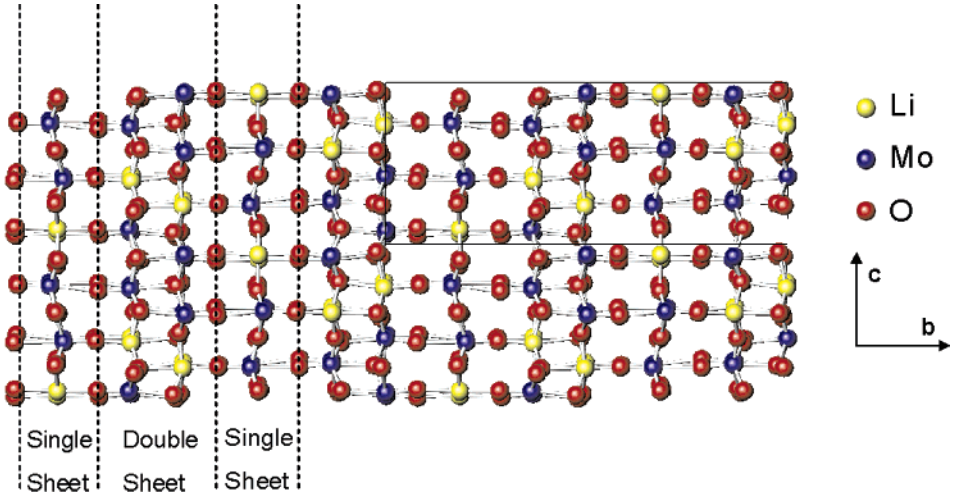

Figure 1. Extended structure of M-$Li_2Mo_4O_{13}$. Starting from left, single sheets alternate with double sheets. The unit cell is outlined in black starting from the right.

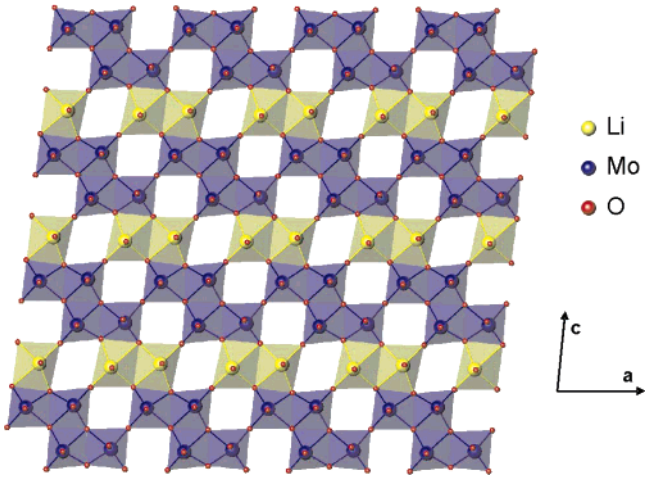

Figure 2. Single-sheet connectivity in M-$Li_2Mo_4O_{13}$. The double sheet is comprised of two single sheets.

coordinate oxygen atoms connect the single sheets to the double sheets. The double sheets in M-$Li_2Mo_4O_{13}$ are built up from two single sheets that are connected by shared oxygen atoms within the sheets. The octahedra of the double sheet have two types of coordination. One coordination environment shares edges with five other octahedra: two octahedra from within the same plane (the single-sheet connectivity described above) and three octahedra from the second sheet. The other coordination environment shares edges with only two octahedra from the second sheet, for a total of four shared edges.

The lithium- and molybdenum-centered octahedra are separated into ordered rows within the crystal framework, and each row of LiO_6 octahedra is separated by two rows of MoO_6 octahedra, which is illustrated within the single sheet shown in Figure 2. The LiO_6 octahedra form a zigzag pattern along the b-axis, leading to the 2_1 screw, depicted in Figure 3a. All of the octahedra are distorted, but bond valence calculations agree with the expected oxidation states of Li^+ and Mo^{6+}. Mo−O

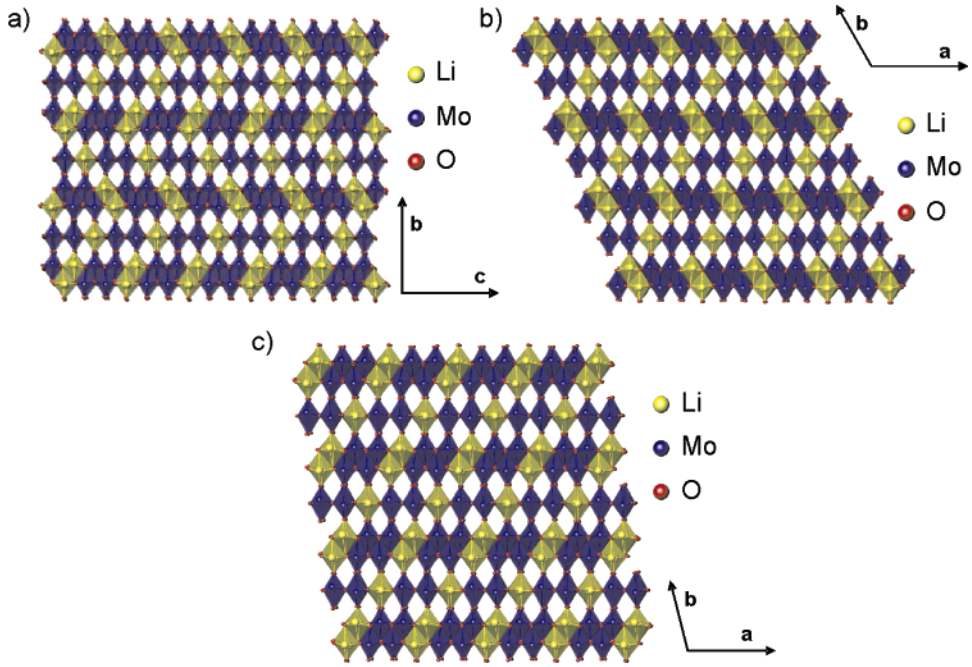

Figure 3. Polyhedral illustration of (a) M-$Li_2Mo_4O_{13}$, (b) H-$Li_2Mo_4O_{13}$, and (c) L-$Li_2Mo_4O_{13}$.

Table 2. Mo−O Bond Distances and Bond Valences[a] in *M*-$Li_2Mo_4O_{13}$

bond	distance (Å)	valence	bond	distance (Å)	valence
Mo(1)−O(1)	1.966(4)	0.852	Mo(7)−O(1)	2.303(7)	0.343
Mo(1)−O(2)	1.714(4)	1.684	Mo(7)−O(20)	1.905(5)	1.005
Mo(1)−O(3)	1.692(5)	1.788	Mo(7)−O(22)	1.708(4)	1.710
Mo(1)−O(4)	2.177(5)	0.483	Mo(7)−O(23)	1.700(6)	1.749
Mo(1)−O(5)	1.949(3)	0.892	Mo(7)−O(24)	2.045(4)	0.688
Mo(1)−O(24)	2.380(6)	0.279	Mo(7)−O(25)	2.158(4)	0.507
Σ		5.978	Σ		6.002
Mo(2)−O(4)	2.276(4)	0.369	Mo(8)−O(3)	2.598(4)	0.154
Mo(2)−O(5)	1.917(4)	0.975	Mo(8)−O(18)	1.909(4)	0.995
Mo(2)−O(6)	1.708(4)	1.712	Mo(8)−O(26)	1.904(5)	1.009
Mo(2)−O(7)	1.704(6)	1.732	Mo(8)−O(27)	1.700(4)	1.745
Mo(2)−O(8)	1.911(4)	0.987	Mo(8)−O(28)	1.709(5)	1.708
Mo(2)−O(32)	2.389(7)	0.272	Mo(8)−O(29)	2.230(4)	0.417
Σ		6.047	Σ		6.028
Mo(3)−O(4)	1.922(5)	0.959	Mo(9)−O(17)	1.921(4)	0.963
Mo(3)−O(8)	2.124(4)	0.557	Mo(9)−O(18)	2.227(4)	0.421
Mo(3)−O(9)	1.739(4)	1.572	Mo(9)−O(23)	2.572(4)	0.166
Mo(3)−O(10)	1.674(5)	1.877	Mo(9)−O(29)	1.899(4)	1.022
Mo(3)−O(11)	1.942(4)	0.913	Mo(9)−O(30)	1.710(7)	1.698
Mo(3)−O(34)	2.521(4)	0.190	Mo(9)−O(31)	1.709(4)	1.707
Σ		6.068	Σ		5.977
Mo(4)−O(7)	2.460(4)	0.224	Mo(10)−O(4)	2.460(6)	0.224
Mo(4)−O(12)	1.718(4)	1.669	Mo(10)−O(24)	1.936(4)	0.923
Mo(4)−O(13)	1.885(5)	1.058	Mo(10)−O(25)	2.104(4)	0.588
Mo(4)−O(14)	1.696(6)	1.773	Mo(10)−O(32)	1.758(5)	1.500
Mo(4)−O(26)	1.989(4)	0.800	Mo(10)−O(33)	1.691(4)	1.792
Mo(4)−O(29)	2.136(4)	0.539	Mo(10)−O(34)	1.930(4)	0.941
Σ		6.063	Σ		5.968
Mo(5)−O(13)	1.893(5)	1.042	Mo(11)−O(9)	2.383(5)	0.276
Mo(5)−O(15)	1.708(4)	1.710	Mo(11)−O(25)	1.938(4)	0.921
Mo(5)−O(16)	1.703(5)	1.734	Mo(11)−O(34)	2.279(4)	0.365
Mo(5)−O(17)	1.978(3)	0.825	Mo(11)−O(35)	1.692(7)	1.788
Mo(5)-O(18)	2.125(4)	0.554	Mo(11)-O(36)	1.725(4)	1.640
Mo(5)−O(33)	2.571(4)	0.166	Mo(11)−O(37)	1.923(4)	0.956
Σ		6.031	Σ		5.946
Mo(6)−O(1)	1.935(4)	0.928	Mo(12)−O(11)	2.405(5)	0.260
Mo(6)−O(8)	2.171(4)	0.491	Mo(12)−O(20)	1.980(4)	0.821
Mo(6)−O(11)	2.048(4)	0.681	Mo(12)−O(34)	2.157(4)	0.509
Mo(6)−O(19)	1.684(6)	1.830	Mo(12)−O(37)	1.932(3)	0.936
Mo(6)−O(20)	2.354(7)	0.299	Mo(12)−O(38)	1.674(4)	1.877
Mo(6)−O(21)	1.709(4)	1.708	Mo(12)−O(39)	1.719(4)	1.660
Σ		5.937	Σ		6.063

[a] Bond valences calculated with the program Bond Valence Calculator v 2.00 (C. Hormillosa, S. Healy, and T. Stephen, McMaster University, 1993).

Table 3. Li−O Bond Distance and Bond Valences[a] in *M*-$Li_2Mo_4O_{13}$

bond	distance (Å)	valence	bond	distance (Å)	valence
Li(1)−O(2)	2.529(10)	0.056	Li(4)−O(2)	2.531(13)	0.056
Li(1)−O(5)	1.994(10)	0.240	Li(4)−O(22)	2.475(8)	0.065
Li(1)−O(9)	2.040(10)	0.212	Li(4)−O(24)	2.053(9)	0.204
Li(1)−O(21)	1.987(10)	0.245	Li(4)−O(28)	1.871(13)	0.334
Li(1)−O(30)	1.897(15)	0.312	Li(4)−O(36)	2.012(9)	0.228
Li(1)−O(36)	2.317(15)	0.100	Li(4)−O(39)	1.965(9)	0.259
Σ		1.165	Σ		1.146
Li(2)−O(2)	1.987(9)	0.244	Li(5)−O(12)	2.044(10)	0.210
Li(2)−O(6)	1.965(9)	0.260	Li(5)−O(15)	2.521(9)	0.058
Li(2)−O(11)	2.029(9)	0.218	Li(5)−O(17)	2.022(10)	0.222
Li(2)−O(16)	1.906(13)	0.305	Li(5)−O(19)	2.239(10)	0.124
Li(2)−O(21)	2.550(8)	0.053	Li(5)−O(27)	1.947(10)	0.273
Li(2)−O(39)	2.444(13)	0.071	Li(5)−O(35)	2.115(11)	0.173
Σ		1.151	Σ		1.060
Li(3)−O(6)	2.388(15)	0.083	Li(6)−O(10)	2.235(10)	0.125
Li(3)−O(14)	1.924(14)	0.290	Li(6)−O(12)	2.415(10)	0.077
Li(3)−O(22)	2.003(10)	0.235	Li(6)−O(15)	2.039(11)	0.213
Li(3)−O(32)	1.982(9)	0.248	Li(6)−O(26)	2.034(11)	0.215
Li(3)−O(37)	2.014(9)	0.228	Li(6)−O(31)	1.978(10)	0.251
Li(3)−O(39)	2.580(9)	0.049	Li(6)−O(38)	2.216(10)	0.132
Σ		1.133	Σ		1.013

[a] Bond valences calculated with the program Bond Valence Calculator v 2.00 (C. Hormillosa, S. Healy, and T. Stephen, McMaster University, 1993).

and Li−O bond lengths and bond valence sums[10,11] are listed in Tables 2 and 3, respectively.

The Mo−O bond lengths of the MoO_6 octahedra vary from ∼1.7 to ∼2.5 Å within each individual octahedron. The long Mo−O bond lengths (∼2.5 Å) donate minimal bonding contributions, and the molybdenum polyhedra show a tendency toward a coordination intermediate between tetrahedral and square pyramidal. Distorted tetrahedral MoO_4 units with two associated weakly bound oxygen atoms are widespread in molybdates as evidenced by compounds such as $Hg_2Mo_5O_{16}$,[12] $Cs_2Mo_5O_{16}$,[13] $Cs_2Mo_7O_{22}$,[13] $Tl_2Mo_4O_{13}$,[14] and $K_2Mo_4O_{13}$.[15] Similarly, and as expected, the LiO_6 octahedra are distorted with Li−O bond lengths in the range from ∼1.9 to ∼2.5 Å. The oxygen coordination varies from two to four. The corner-shared oxygen atoms between the single and double sheets are two-coordinate, while the oxygen atoms connecting the double sheet are three- and four-coordinate.

3.2. Structural Relationships among V_6O_{13}, M-$Li_2Mo_4O_{13}$, H-$Li_2Mo_4O_{13}$, and L-$Li_2Mo_4O_{13}$. *M*-$Li_2Mo_4O_{13}$ is a homeotype of V_6O_{13}. V_6O_{13} can be derived from V_2O_5 by removal of the atoms on every third (001) oxygen atom plane followed by the 1/6[1 0 −3] crystallographic shear.[16] As recognized previously, the crystallographic shear plane is part of a cubic close-packed oxygen lattice with regular oxygen vacancies.[2] Two out of every 15 oxygen atoms are vacant in the close-packed oxygen array

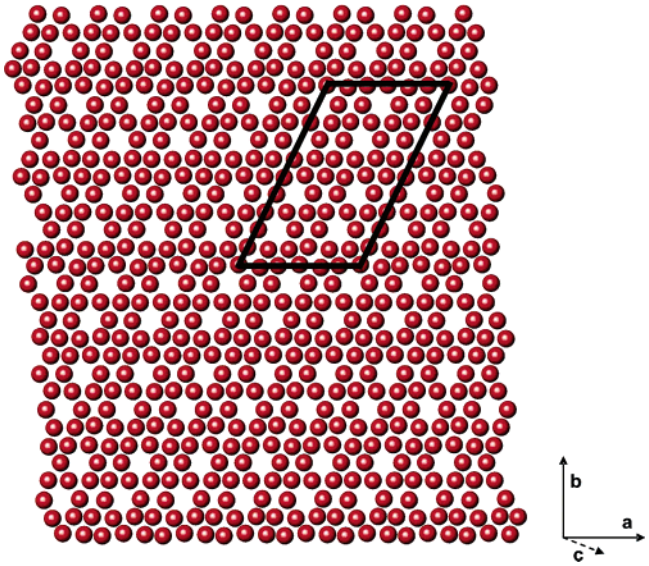

Figure 4. Close-packed oxygen array in *M*-$Li_2Mo_4O_{13}$. The oxygen plane can be extracted from Figure 3a by slicing parallel to the *a*-axis and bisecting the *b* and *c* axes. Two out of every 15 oxygen atoms are vacant, as illustrated by the repeating unit given by the outline (atoms or vacancies at the corner of the outline are counted as a quarter and atoms or vacancies on the line are counted as a half).

after the shear plane is formed, and V_2O_5, or V_6O_{15}, simply becomes $V_6O_{13}\square_2$, where □ represents a regular oxygen vacancy in the close-packed oxygen array. Therefore, while the shear plane is an effective explanation for the structural transformation from V_2O_5 to V_6O_{13}, it also results in what is simply a face-centered cubic oxygen array with 2 of every 15 oxygen sites vacant, as shown in Figure 4. Octahedral sites are occupied by either lithium or molybdenum cations, shown in Figure 5, for the three polymorphs.

The three polymorphs of $Li_2Mo_4O_{13}$ are each homeotypic parent-derivative pairs[2,3] with V_6O_{13}. In the $Li_2Mo_4O_{13}$ phases, two lithium and four molybdenum atoms cosubstitute for the six vanadium atoms, and a unique distribution of lithium and molybdenum gives rise to the three distinct phases that can be seen in Figure 3. The structural frameworks are the same because each individual sheet is identical for all three phases,

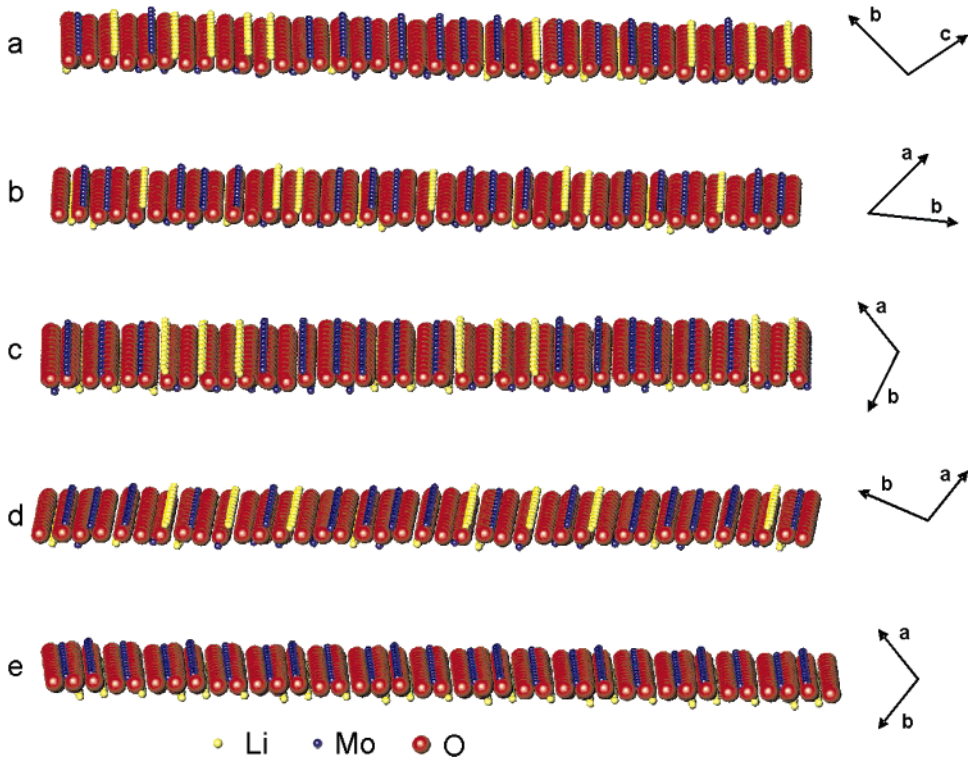

Figure 5. Ordered rows of Li^+ and Mo^{6+} fill the octahedral positions. Octahedral filling in (a) *M*-$Li_2Mo_4O_{13}$, (b) and (c) *H*-$Li_2Mo_4O_{13}$, and (d) and (e) *L*-$Li_2Mo_4O_{13}$.

shown in Figure 2. The sheets should not be confused with the close-packed layers because the sheets simply reflect the octahedral filling of the close-packed layering. The extended structures of the three $Li_2Mo_4O_{13}$ polymorphs differ, owing to the octahedral filling within the close-packed layers, and examination of the close-packed layers reveals why the three polymorphs evolve. Each polymorph has a close-packed oxygen array with 2 of every 15 oxygen atoms vacant and ordered rows of lithium or molybdenum filling the octahedral sites. As previously mentioned and depicted in Figure 5a, each close-packed oxygen layer in *M*-$Li_2Mo_4O_{13}$ fills the octahedral sites according to ordered rows of −(7Mo−4Li−1Mo−1Li−4Mo−1Li)−, whether along the [011] direction or the [01−1] direction. Figure 5 also displays the perpendicular close-packed layers and octahedral filling for *H*- $Li_2Mo_4O_{13}$ in Figures 5b, −(3Mo−2Li−3Mo−1Li)−, and 5c, −(6Mo−3Li)−, and *L*-$Li_2Mo_4O_{13}$ in Figures 5d, −(4Mo−1Li−1Mo−1Li−1Mo−1Li)−, and 5e (either all Mo or all Li). These individual octahedral filling patterns lead to the three polymorphs shown in Figure 3. As is later discussed, these polymorphs can be transformed among themselves as the cations likely move to accommodate bond valences. When one focuses on a common stoichiometry and framework, such as a close-packed oxygen array, many potential cosubstituted structures with other cation combinations can be envisioned.

3.3. Relative Stability of M-$Li_2Mo_4O_{13}$. *M*-$Li_2Mo_4O_{13}$ is unstable at room temperature and slowly transforms into *H*-$Li_2Mo_4O_{13}$. That is, after 3 months, the crystals of *M*-$Li_2Mo_4O_{13}$ that were used for the single-crystal X-ray analysis had transformed into single crystals of *H*-$Li_2Mo_4O_{13}$ which were also suitable single crystals. Presumably, a single crystal is maintained because the anion framework of the two phases is identical, and a cation migration mechanism is likely. *H*-$Li_2Mo_4O_{13}$ is the thermodynamically stable form at room temperature. *L*-$Li_2Mo_4O_{13}$ will also transform into the high-temperature phase.[1] Because each of the $Li_2Mo_4O_{13}$ phases are derivatives of the same structure with similar metal−anion, metal−metal, and anion−anion energetics, the energy difference between the three structures is minimal. Nonetheless, the conversion of the kinetic *M* and *L* phases into the thermodynamic *H* phase is a relatively slow process, which makes possible the detailed structural characterization of the kinetic products. The synthesis conditions (temperature, melt composition, heating and cooling rate, etc.) are what likely determine the kinetic crystallization product.

In a description of a possible transformation mechanism from *L*-$Li_2Mo_4O_{13}$ to *H*-$Li_2Mo_4O_{13}$, *M*-$Li_2Mo_4O_{13}$ was excluded as a possible intermediate because the 2_1 screw axis is inconsistent with V_6O_{13}.[3] However, in light of the current crystallographic structure determination and the interrelated structures of the three polymorphs, further investigations are warranted to determine the transformation pathways.

4. Conclusions

The structure of *M*-$Li_2Mo_4O_{13}$, a third polymorph of $Li_2Mo_4O_{13}$, has been determined. *M*-$Li_2Mo_4O_{13}$, *H*-$Li_2Mo_4O_{13}$, and *L*-$Li_2Mo_4O_{13}$ are polymorphs and are cosubstituted V_6O_{13} homeotypes constructed from a common oxygen-deficient $V_6O_{13}\square_2$ close-packed oxygen framework. The polymorphs differ in their occupation patterns of the octahedral sites within this oxygen-deficient cubic close-packed oxygen array. Additionally, *M*-$Li_2Mo_4O_{13}$ is unstable at room temperature and slowly transforms to *H*-$Li_2Mo_4O_{13}$.

Acknowledgment. The authors gratefully acknowledge the National Science Foundation, Solid State Chemistry (Award Nos. DMR-0312136 and DMR-0604454), the EMSI program of the National Science Foundation at the Northwestern University Institute for Environmental Catalysis (Grant No.

9810378), and the Department of Energy, BES-Chemical Sciences, Geosciences, and Biosciences Division under Grant No. DE-FG0203ER15457, and the use of the Central Facilities supported by the MRSEC program of the National Science Foundation (DMR-0576097) at the Materials Research Center of Northwestern University.

Supporting Information Available: An X-ray crystallographic file in CIF format and a table of atomic positions and displacement parameters. This material is available free of charge via the Internet at http://pubs.acs.org.

References

(1) Brower, W. S.; Parker, H. S.; Roth, R. S.; Waring, J. L. *J. Cryst. Growth* **1972**, *16*, 115−120.
(2) Gatehouse, B. M.; Miskin, B. K. *J. Solid State Chem.* **1974**, *9*, 247−254.
(3) Gatehouse, B. M.; Miskin, B. K. *J. Solid State Chem.* **1975**, *15*, 274−282.
(4) Wilhelmi, K. A.; Waltersson, K.; Kihlborg, L. *Acta Chem. Scand.* **1971**, *25*, 2675−2687.
(5) Smit, J. P.; Stair, P. C.; Poeppelmeier, K. R. *Chem.−Eur. J.* **2006**, *12*, 5944−5953.
(6) SAINT-Plus, 6.02A; Bruker Analytical X-Ray Instruments, Inc.: Madison, WI, 2000.
(7) SADABS, 2.05; Bruker Analytical X-Ray Instruments, Inc.: Madison, WI, 2003.
(8) Spek, A. L. *J. Appl. Crystallogr.* **2003**, *36*, 7−13.
(9) Sheldrick, G. M. *SHELXTL*, 6.14; Bruker Analytical X-Ray Instruments, Inc.: Madison, WI, 2003.
(10) Brown, I. D.; Altermatt, D. *Acta Crystallogr., Sect. B: Struct. Sci.* **1985**, *B41*, 244−247.
(11) Brese, N. E.; O'Keeffe, M. *Acta Crystallogr., Sect. B: Struct. Sci.* **1991**, *B47*, 192−197.
(12) Wessels, A. L.; Jeitschko, W. *J. Solid State Chem.* **1997**, *128*, 205−208.
(13) Gatehouse, B. M.; Miskin, B. K. *Acta Crystallogr., Sect. B* **1975**, *B31*, 1293−1299.
(14) Kini, M. R.; Udupa, M. R.; Aravamudan, G. *Curr. Sci.* **1973**, *42*, 536−537.
(15) Leverett, P.; Gatehouse, B. M. *J. Chem. Soc. A* **1971**, 2107−2112.
(16) Ohno, T.; Nakamura, Y.; Nagakura, S. *J. Solid State Chem.* **1985**, *56*, 318−324.

CG060576L